TL 112-00/00

L.O. 6107A FILE BM2-1-64 PREPARED BY D.G.G. CHECKED BY A.D.W.	NATIONAL AERONAUTICAL ESTABLISHMENT ARNPRIOR, CANADA LABORATORY MEMORANDUM SECTION FLIGHT RESEARCH	NO FR-10(b) PAGE COPY NO. 9 DATE 3 February, 19

SECURITY CLASSIFICATION ~~SECRET~~ UNCLASSIFIED

SUBJECT

PRESSURE MEASUREMENTS ON THE UPPER AND LOWER SURFACE OF THE NACELLE-FUSELAGE FILLET OF THE AVRO CF-100 HALF MODEL

PREPARED BY

D. G. GOULD

ISSUED TO

INTERNAL

SUMMARY

The chordwise variation of the pressure coefficient along the upper and lower surface of the fuselage-nacelle fillet of the Avro CF-100 half model was obtained over the Mach number range from 0.53 to 0.99 at angles of attack of 0°, 2°, 4° and 6°.

The chordwise position of the forward suction peak on the upper surface was invariant with Mach number. A second suction peak occurred on the upper surface at Mach numbers above 0.80. The position of the second peak moved aft from the 35% chord position at $M = 0.80$ to the 70% chord position at $M = 0.99$.

The pressure distribution on the lower surface, aft of the 10% chord position, was approximately flat at all Mach numbers up to $M = 0.72$. At higher Mach numbers a second peak occurred. This peak moved rapidly aft from the 35% chord position at $M = 0.82$ to the 55% chord position at $M = 0.86$.

1. INTRODUCTION

In Reference 1 the results are presented of total head wake surveys behind the nacelle fillet, nacelle and inboard wing of a 1/80 scale model of the CF-100. To supplement this information surface static pressure distributions have been made. This memorandum presents the results of surface static pressure measurements made along the upper and lower surface of the nacelle fillet. The upper surface distributions are compared with those obtained at much higher Reynolds Numbers by the Cornell Aeronautical Laboratory. The lower surface distributions are of particular interest in determining a suitable location for external stores on this aircraft.

2. SCOPE OF TESTS

Chordwise pressure distributions were obtained along the upper and lower surface of the fuselage-nacelle fillet over a range of Mach numbers from 0.53 to 0.99, at angles of attack (measured from the fuselage reference line) of 0°, 2°, 4°, and 6°. The corresponding range of Reynold's numbers was from 0.17×10^6 to 0.33×10^6 based on the S.M.C. (Figure 1).

3. APPARATUS

The N.A.E. transonic wing flow facilities were used to conduct the tests.

Nine pressure orifices, 0.040 inches in diameter, were located chordwise along both the upper and lower surfaces of the fuselage-nacelle fillet.

The pressures were recorded using a multi-channel pressure recorder (M-2).

4. METHOD

A steady Mach number was established in the flow past the model and the model cycled through six degrees angle of attack in two degree steps, with the model pausing 1½ seconds at each step.

All tests were carried out in level flight or in shallow dives so that lag effects were considered negligible.

5. RESULTS

The results are presented in Figures 2 to 22 as the chordwise variation of the pressure coefficient, $C_p = \frac{P_s - P_{os}}{q_o}$

The pressure distributions from Reference 2 indicate that the pressure peak on the upper surface is generally forward of the 5% chord position. Since the most forward orifice in the present tests was located at 5.5% of the chord, the curves were not extended forward of this position.

The chordwise pressure distributions along the upper surface of the fillet, for Mach numbers from 0.53 to 0.99 are shown in Figures 2 to 11. The pressure distributions are approximately invariant with Mach number up to $M = 0.75$. (Figures 2 to 6). The suction peak occurs somewhere forward of the 5.5% chord position; the pressure increasing rapidly back to about 10% chord and then increasing more or less linearly back to 80% chord position.

At $M = 0.80$ (Figure 7) a second suction peak occurs at the 35% chord position for angles of attack up to 4°. As the Mach number is increased beyond $M = 0.80$, the second suction peak moves aft with increasing Mach number to the 70% chord position at $M = 0.99$ (Figures 8 to 11). It appears that separation of the boundary layer well forward on the surface occurs at $\alpha = 6^\circ$ for all Mach numbers from $M = 0.80$ to $M = 0.93$. At $M = 0.99$ there is no evidence of early separation at $\alpha = 6^\circ$.

It seems likely that the second suction peak occurring at Mach numbers greater than $M = 0.80$ is associated with a rapid thickening of the boundary layer due to transition caused by the shock wave behind the forward suction peak. Alternately, the boundary layer may be separated by the shock wave and reattaches itself as a turbulent boundary layer farther aft. There is evidence of a second shock occurring behind the second suction peak at Mach numbers greater than $M = 0.88$.

An accurate estimate of the critical Mach number of the upper surface of the fillet is difficult since the suction peak probably occurs forward of the 5.5% chord position. It is evident, however, from Figure 4 that the critical Mach number at lift coefficients above 0.45 is less than $M = 0.62$. This agrees reasonably well with the data from Reference 2; the critical Mach number of the fuselage-nacelle fillet being 0.57 at $C_L = 0.45$.

Pressure distributions along the lower surface of the fuselage-nacelle fillet are given in Figures 12 to 22 over the Mach number range from M = 0.53 to M = 0.99. At Mach numbers below 0.72 there is little change in the pressure distribution with Mach number (Figures 12 to 15). The suction peak occurs at the 5% chord position or farther forward; the pressure increases rapidly back to 10% chord and is approximately flat from 10% chord to 80% chord. At M = 0.82 a second suction peak occurs at $\alpha = 0^\circ$ at the 35% chord position (Figure 16). This peak moves rapidly aft with increasing Mach number to the 55% chord position at M = 0.86.

The critical Mach number of the lower surface at $\alpha = 0^\circ$ appears to be at about M = 0.72. Figure 18 indicates that the critical pressure coefficient is not reached on the lower surface at $\alpha = 6^\circ$ until M = 0.86.

Pressure distributions along the upper surface of the fillet obtained from the present tests are compared with those of Reference 2 in Figures 23 and 24. The results are compared at lift coefficients of 0.09 and 0.62 at a Mach number of approximately 0.5 in Figure 23. The agreement is reasonably good, especially aft of the 15% chord position. The difference in the magnitude of the suction peak at the lower lift coefficient could be accounted for by a difference of .01 in the lift coefficient. The lift coefficient in the present tests was not known to an accuracy of better than ± .015.

The comparison at M = 0.88 given in Figure 24 shows a marked discrepancy between the results at a lift coefficient of 0.32. At $C_L = .06$ the agreement is fair except for the portion aft of the 50% chord position; where the data from Reference 2 indicates considerably more suction than the present tests. According to the present results at M = 0.88, as the angle of attack was increased from 0° to 6° the magnitude of the second suction peak decreased. Reference 2 shows that at M = 0.88, as the angle of attack was increased, the magnitude of the second suction peak increased. Thus there is a large difference in the magnitude of the second suction peak between the two sets of data at a lift coefficient of 0.32, as shown by Figure 24.

The decrease in the second suction peak with increasing angle of attac found from the present tests seemsprobable if separation caused by the shock following the forward suction peak becomes more severe with increasing angle of attack; the expansion following the forward shock becoming correspondingly less.

It is felt that the results of Reference 2 may be questionable at high Mach numbers since the model frontal area at zero angle of attack is more than 1% of the tunnel area. The critical area ratio for choking conditions at M = 0.88 is 0.987 (from isentropic flow relations). The conditions at angles of attack are, of course, even more critical.

Figure 24 shows a further discrepancy between the two sets of data at $C_L = 0.32$ in the magnitude of the forward suction peak. The relatively large orifice diameter used in the present tests, necessary to keep lag effects

Pressure distributions along the lower surface of the fuselage-nacelle fillet are given in Figures 12 to 22 over the Mach number range from $M = 0.53$ to $M = 0.99$. At Mach numbers below 0.72 there is little change in the pressure distribution with Mach number (Figures 12 to 15). The suction peak occurs at the 5% chord position or farther forward; the pressure increases rapidly back to 10% chord and is approximately flat from 10% chord to 80% chord. At $M = 0.82$ a second suction peak occurs at $\alpha = 0^\circ$ at the 35% chord position (Figure 16). This peak moves rapidly aft with increasing Mach number to the 55% chord position at $M = 0.86$.

The critical Mach number of the lower surface at $\alpha = 0^\circ$ appears to be at about $M = 0.72$. Figure 18 indicates that the critical pressure coefficient is not reached on the lower surface at $\alpha = 6^\circ$ until $M = 0.86$.

Pressure distributions along the upper surface of the fillet obtained from the present tests are compared with those of Reference 2 in Figures 23 and 24. The results are compared at lift coefficients of 0.09 and 0.62 at a Mach number of approximately 0.5 in Figure 23. The agreement is reasonably good, especially aft of the 15% chord position. The difference in the magnitude of the suction peak at the lower lift coefficient could be accounted for by a difference of .01 in the lift coefficient. The lift coefficient in the present tests was not known to an accuracy of better than $\pm$ .015.

The comparison at $M = 0.88$ given in Figure 24 shows a marked discrepancy between the results at a lift coefficient of 0.32. At $C_L = .06$ the agreement is fair except for the portion aft of the 50% chord position; where the data from Reference 2 indicates considerably more suction than the present tests. According to the present results at $M = 0.88$, as the angle of attack was increased from 0° to 6° the magnitude of the second suction peak decreased. Reference 2 shows that at $M = 0.88$, as the angle of attack was increased, the magnitude of the second suction peak increased. Thus there is a large difference in the magnitude of the second suction peak between the two sets of data at a lift coefficient of 0.32, as shown by Figure 24.

The decrease in the second suction peak with increasing angle of attac found from the present tests seemsprobable if separation caused by the shock following the forward suction peak becomes more severe with increasing angle of attack; the expansion following the forward shock becoming correspondingly less.

It is felt that the results of Reference 2 may be questionable at high Mach numbers since the model frontal area at zero angle of attack is more than 1% of the tunnel area. The critical area ratio for choking conditions at $M = 0.88$ is 0.987 (from isentropic flow relations). The conditions at angles of attack are, of course, even more critical.

Figure 24 shows a further discrepancy between the two sets of data at $C_L = 0.32$ in the magnitude of the forward suction peak. The relatively large orifice diameter used in the present tests, necessary to keep lag effects

to a minimum, would probably affect the flow near the leading edge to a greater extent than elsewhere on the surface.

6. CONCLUSIONS

The measured pressure distributions over the upper surface of the fuselage-nacelle fillet indicate that the chordwise position of the forward suction peak is invariant with Mach Number over the range from $M = 0.53$ to $M = 0.99$. A second suction peak occurs for Mach Numbers of $M = 0.80$ and above. The second suction peak moves aft with increasing Mach number from 35% chord at $M = 0.80$ to 70% of the chord at $M = 0.99$. The critical Mach Number of the upper surface is less than $M = 0.68$ at a lift coefficient of 0.10 ($\alpha = 0^\circ$), and less than $M = 0.62$ at lift coefficients above 0.45 ($\alpha > 4^\circ$).

The pressure distribution on the lower surface of the fillet is approximately flat aft of the 10% chord position at all Mach Numbers up to $M = 0.72$. At $M = 0.82$ there is a small second suction peak occurring at $\alpha = 0^\circ$, at about the 35% chord position. This peak moves rapidly aft with increasing Mach Number to the 55% chord position at $M = 0.86$. It remains at the 55% chord position as the Mach Number increases to $M = 0.91$, and then moves aft with increasing Mach Number.

The critical Mach Number of the lower surface at $\alpha = 0^\circ$ is approximately 0.72; at $\alpha = 2^\circ$ and $\alpha = 4^\circ$ the critical Mach Number is less than $M = 0.82$; at $\alpha = 6^\circ$ the critical Mach Number is $M = 0.86$.

The comparison between the present results with those of Reference 2 showed good agreement at $M = 0.50$ at both high and low lift coefficients. At $M = 0.88$, the agreement was fair at $C_L = .09$ but large discrepancies occurred as the lift coefficient was increased. The most marked difference occurred in the magnitude of the second suction peak; the results of the present tests showing a decrease in the magnitude of the second suction peak with increasing angle of attack, with the results from Reference 2 showing an increase in the second suction peak with increasing angle of attack.

REFERENCES

1. NAE Laboratory Memorandum FR-10(a)

2. Cornell Aeronautical Laboratory Report No. AA-597-W-1

FIG · 1

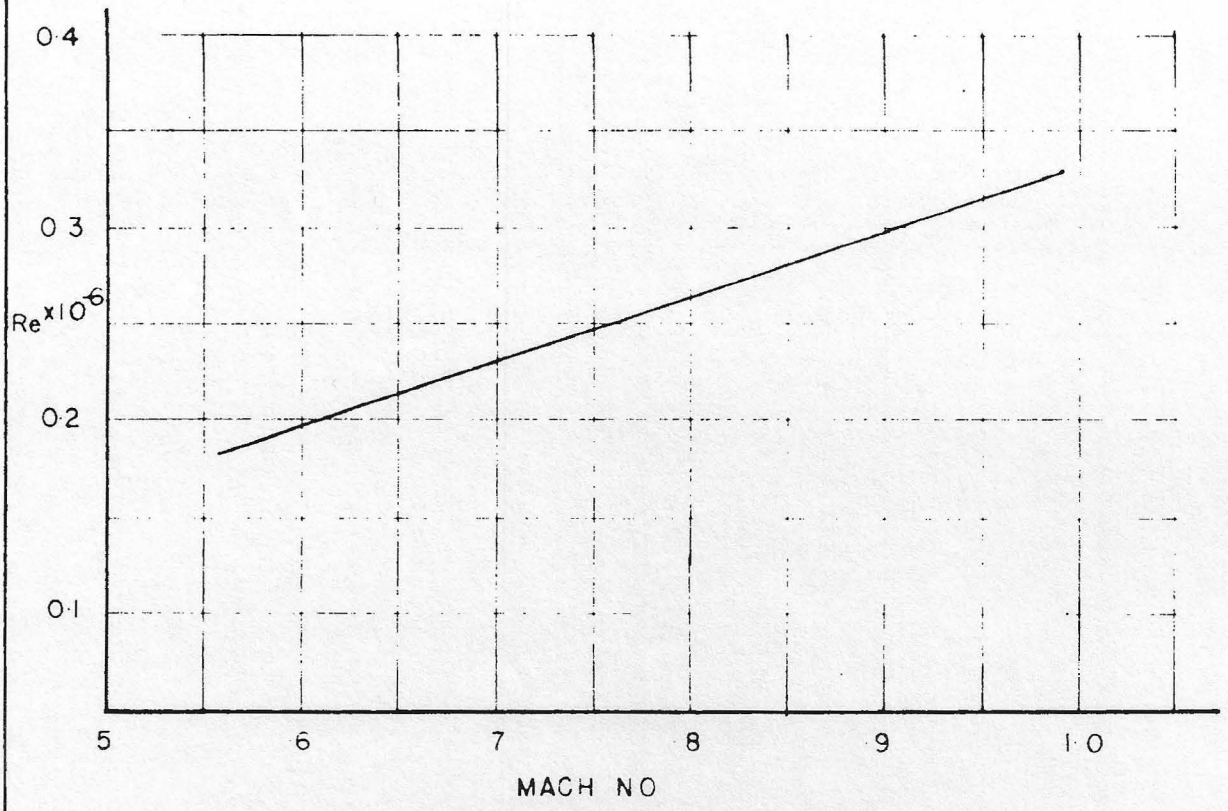

APPROXIMATE VARIATION OF REYNOLDS NUMBER

(BASED ON $\bar{c}$ = 1·56 IN·) WITH MACH NUMBER

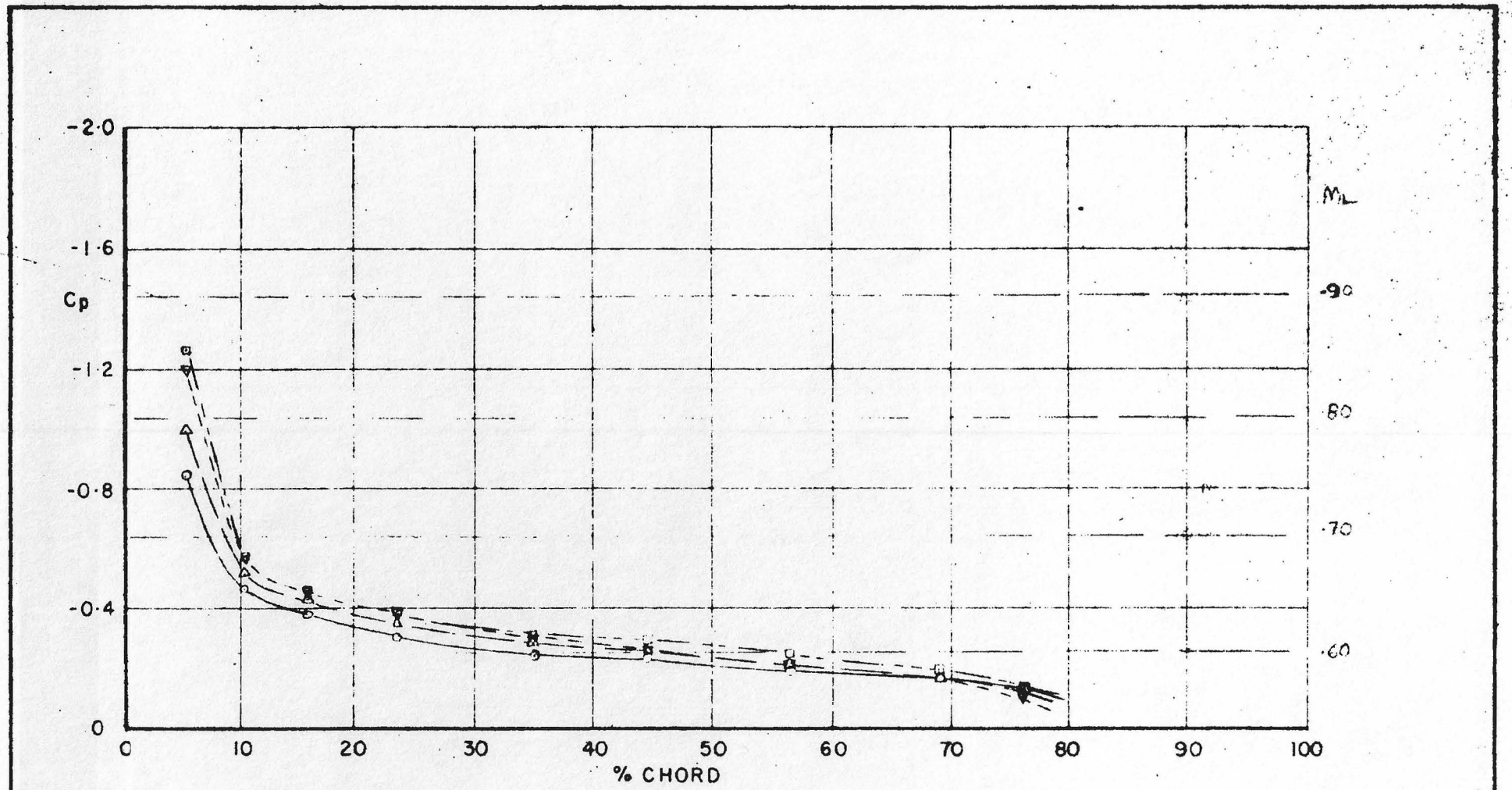

PRESSURE DISTRIBUTION ALONG FUSELAGE-NACELLE FILLET-UPPER SURFACE

M = 0·63

FIG 2

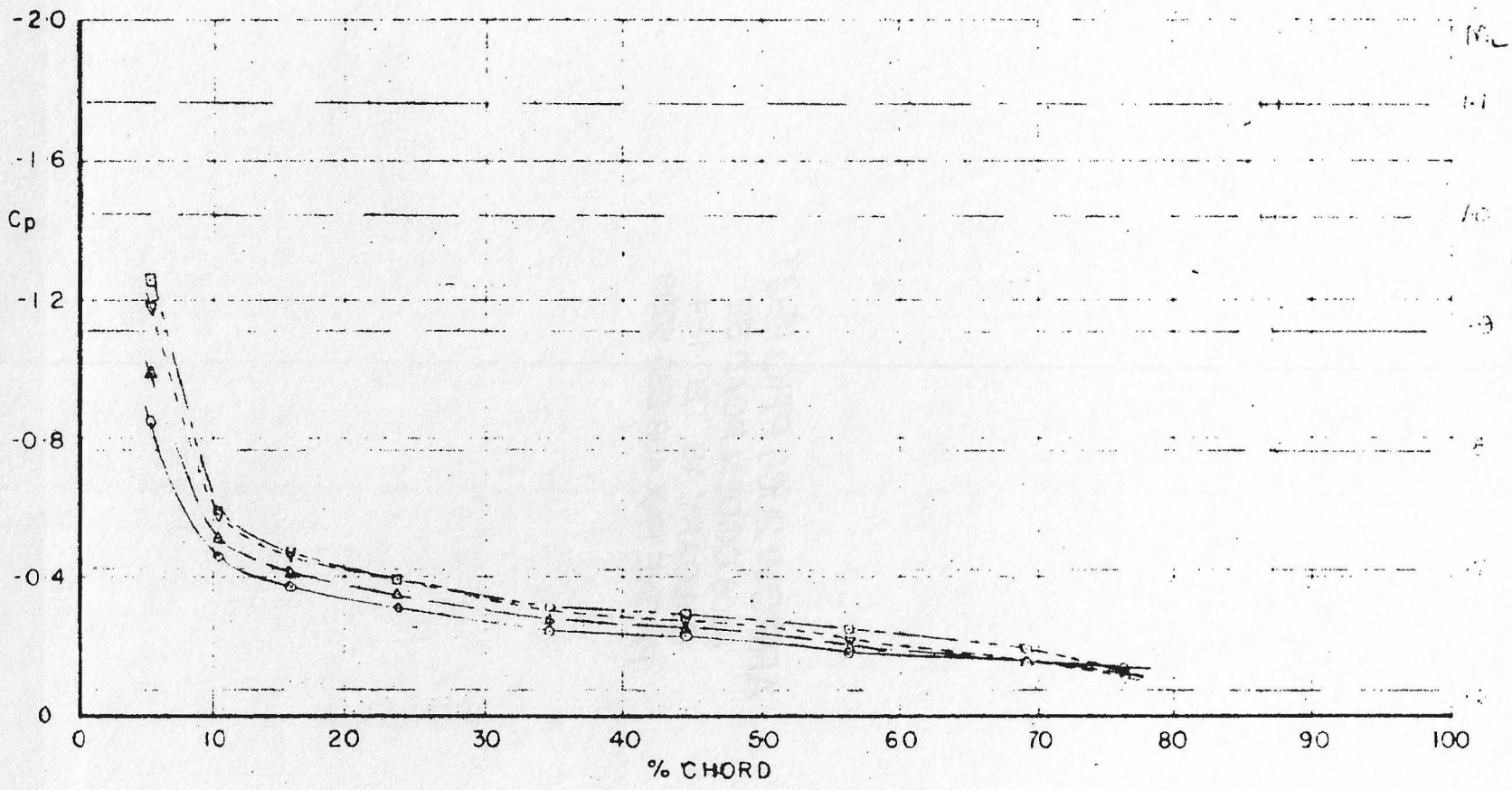

PRESSURE DISTRIBUTION ALONG FUSELAGE-NACELLE FILLET-UPPER SURFACE

M = 58

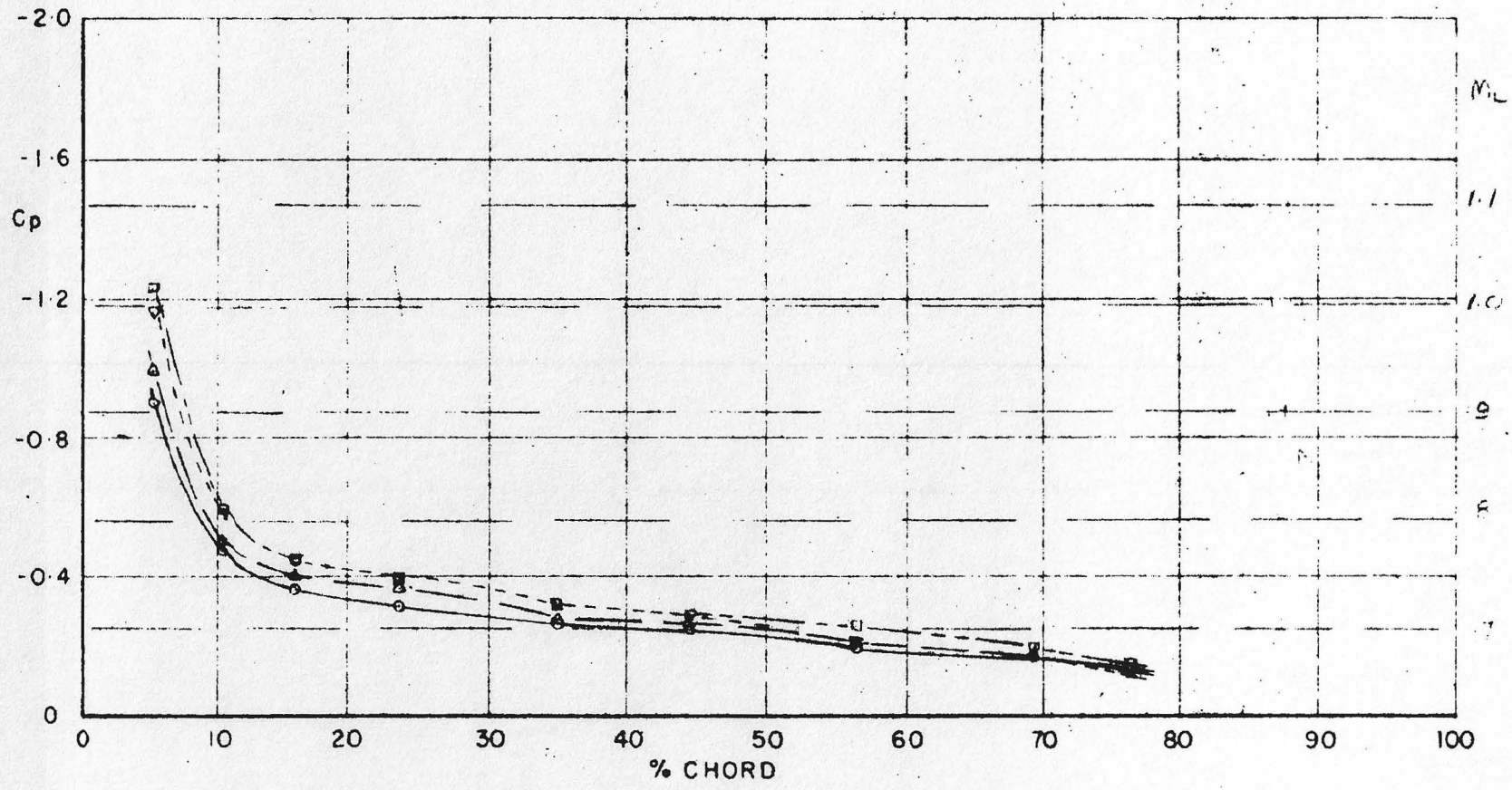

PRESSURE DISTRIBUTION ALONG FUSELAGE-NACELLE FILLET-UPPER SURFACE

M = 0.62

FIG 4

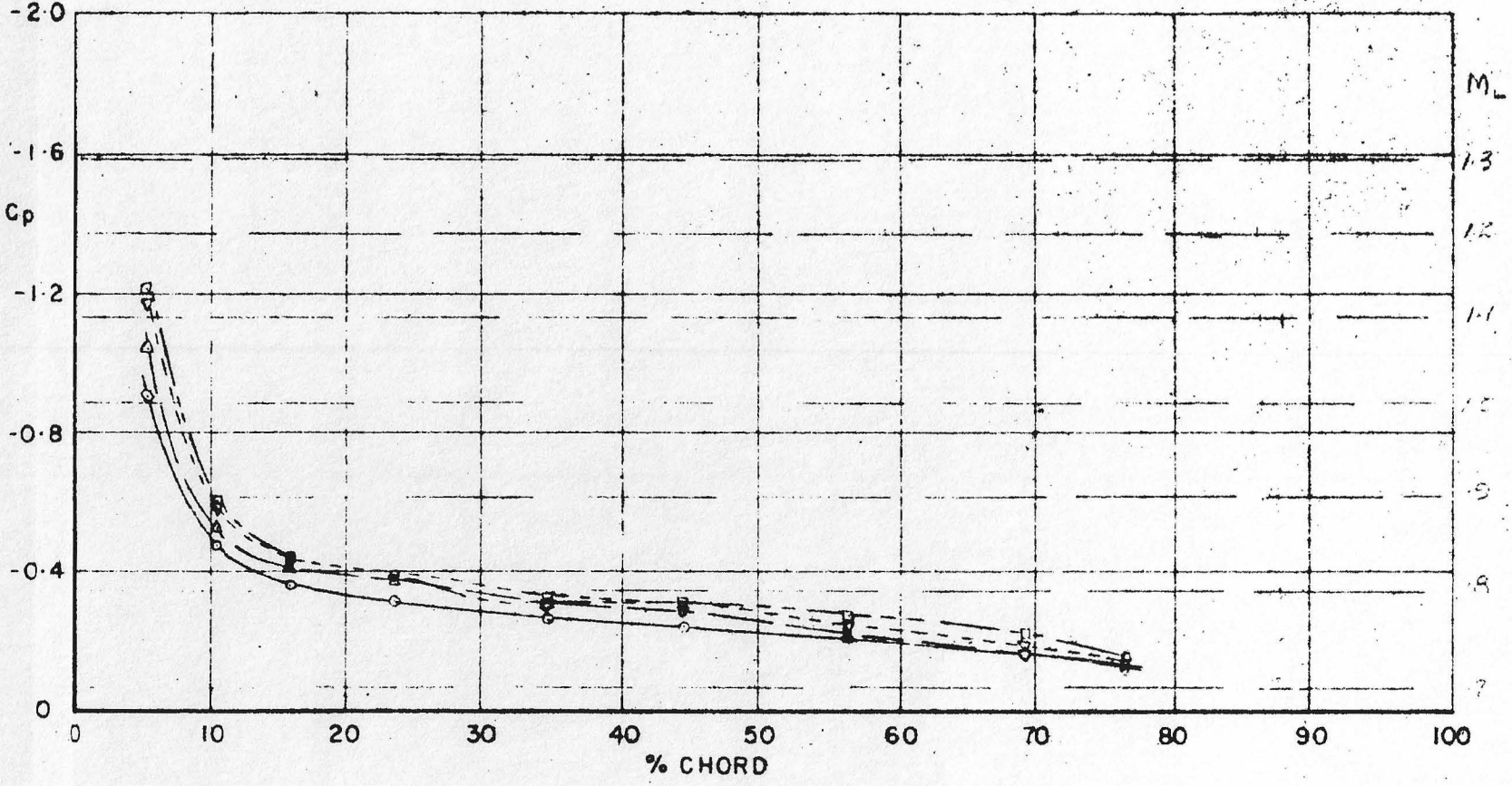

PRESSURE DISTRIBUTION ALONG FUSELAGE-NACELLE FILLET-UPPER SURFACE

M = 0·66

S 514

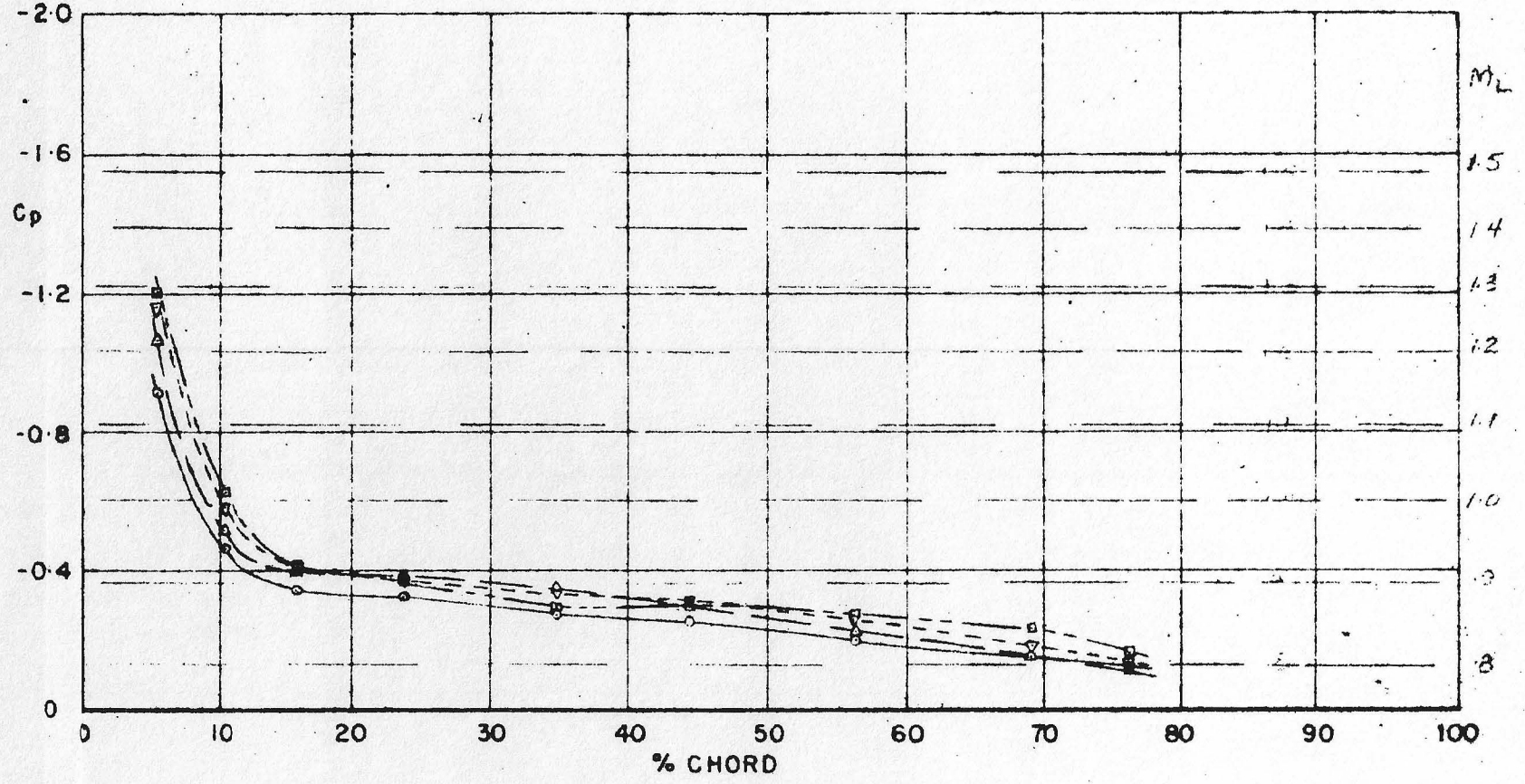

PRESSURE DISTRIBUTION ALONG FUSELAGE-NACELLE FILLET-UPPER SURFACE

M = 0·75

FIG 9

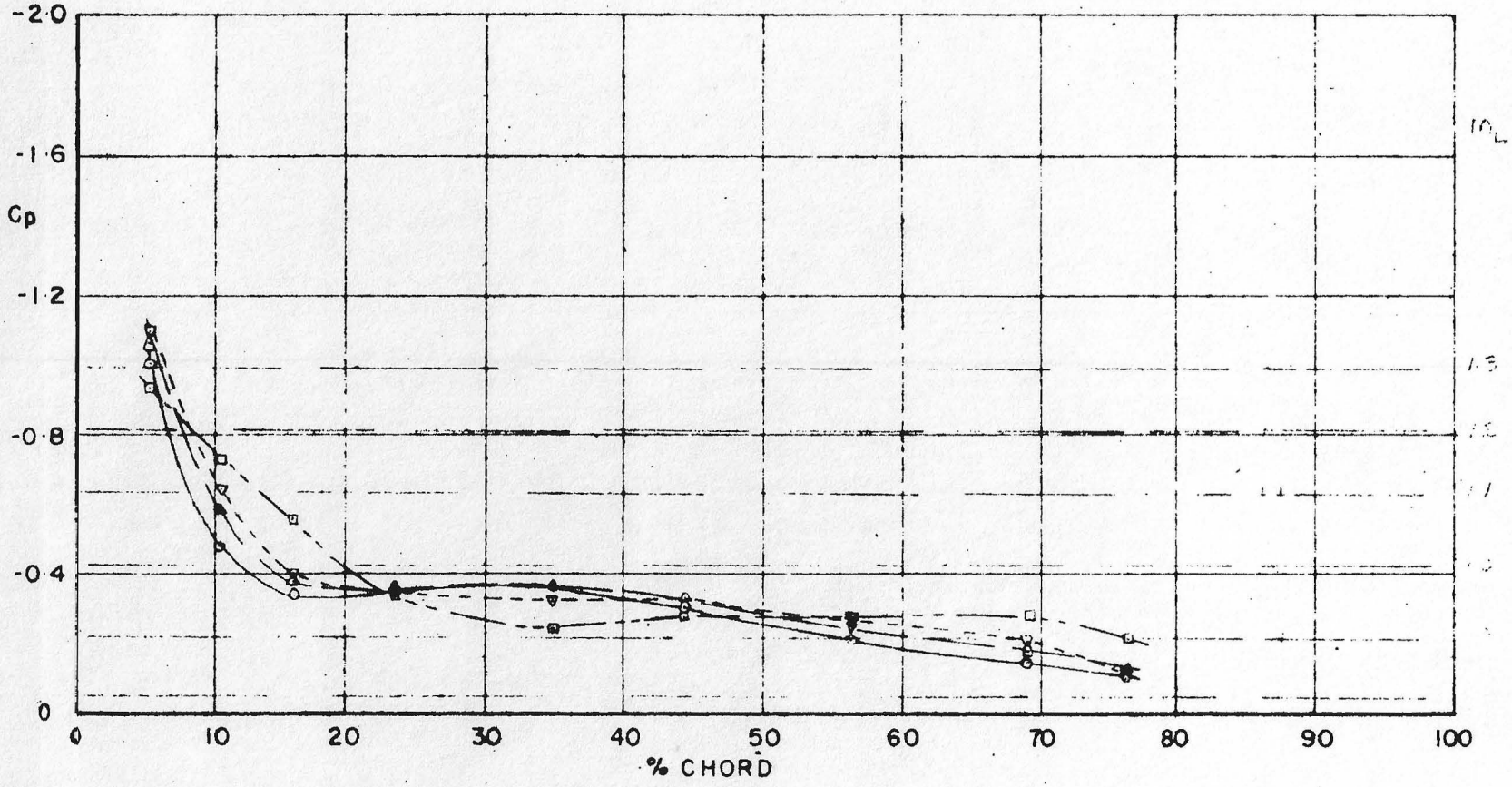

PRESSURE DISTRIBUTION ALONG FUSELAGE-NACELLE FILLET-UPPER SURFACE

M = 0·80

L 514

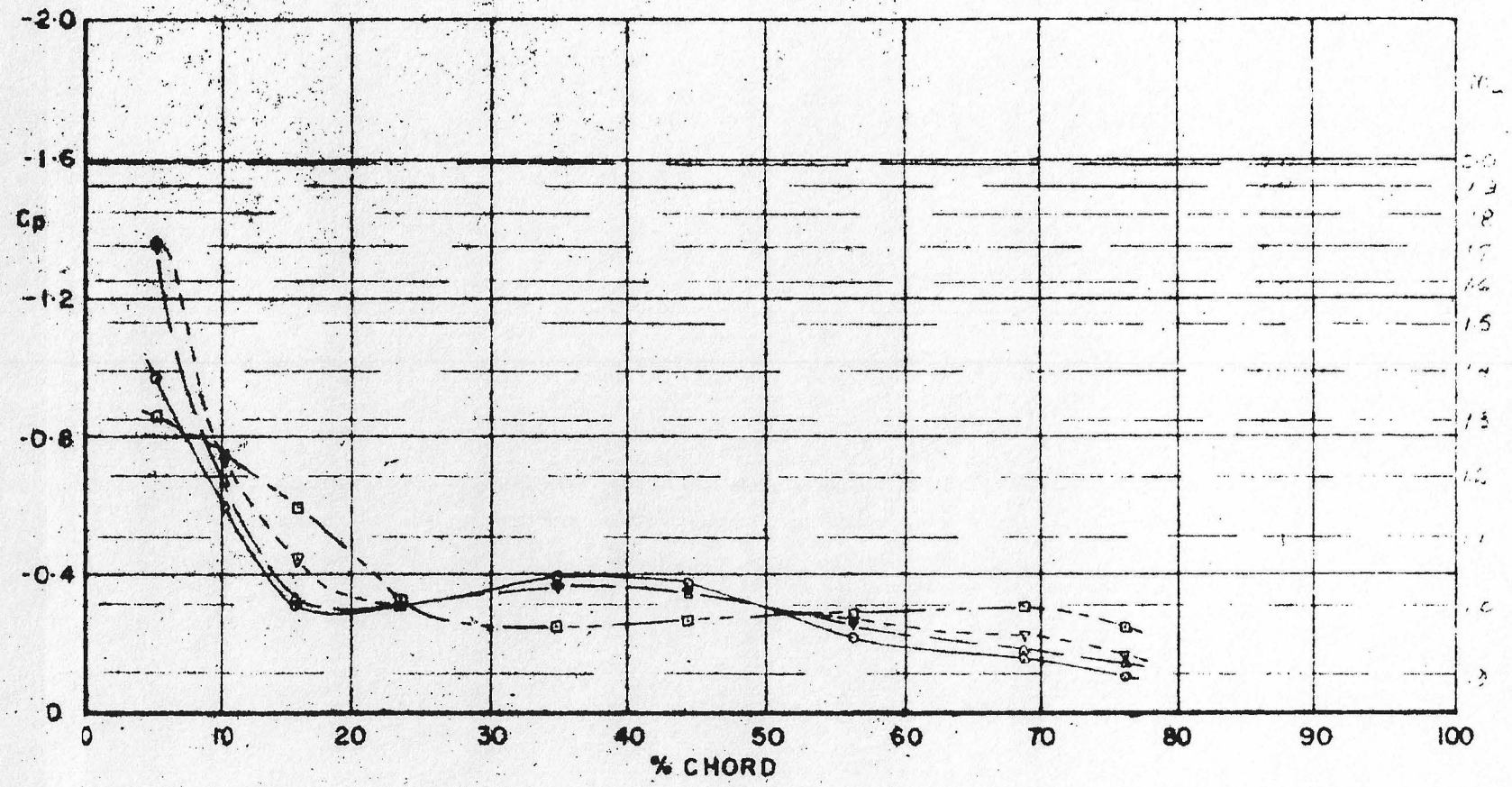

PRESSURE DISTRIBUTION ALONG FUSELAGE-NACELLE FILLET-UPPER SURFACE

M = ·85

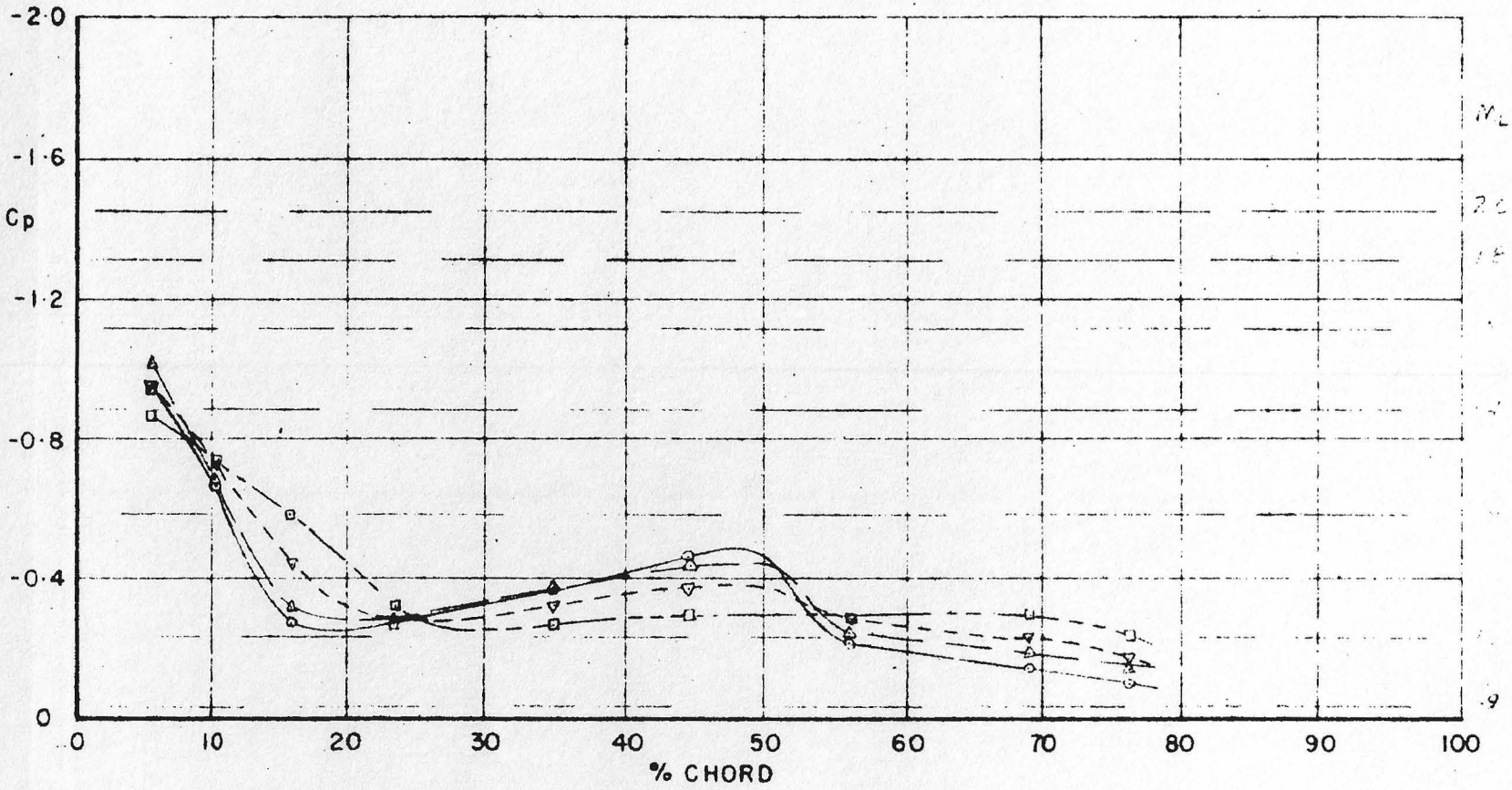

PRESSURE DISTRIBUTION ALONG FUSELAGE-NACELLE FILLET-UPPER SURFACE

M = 0.85

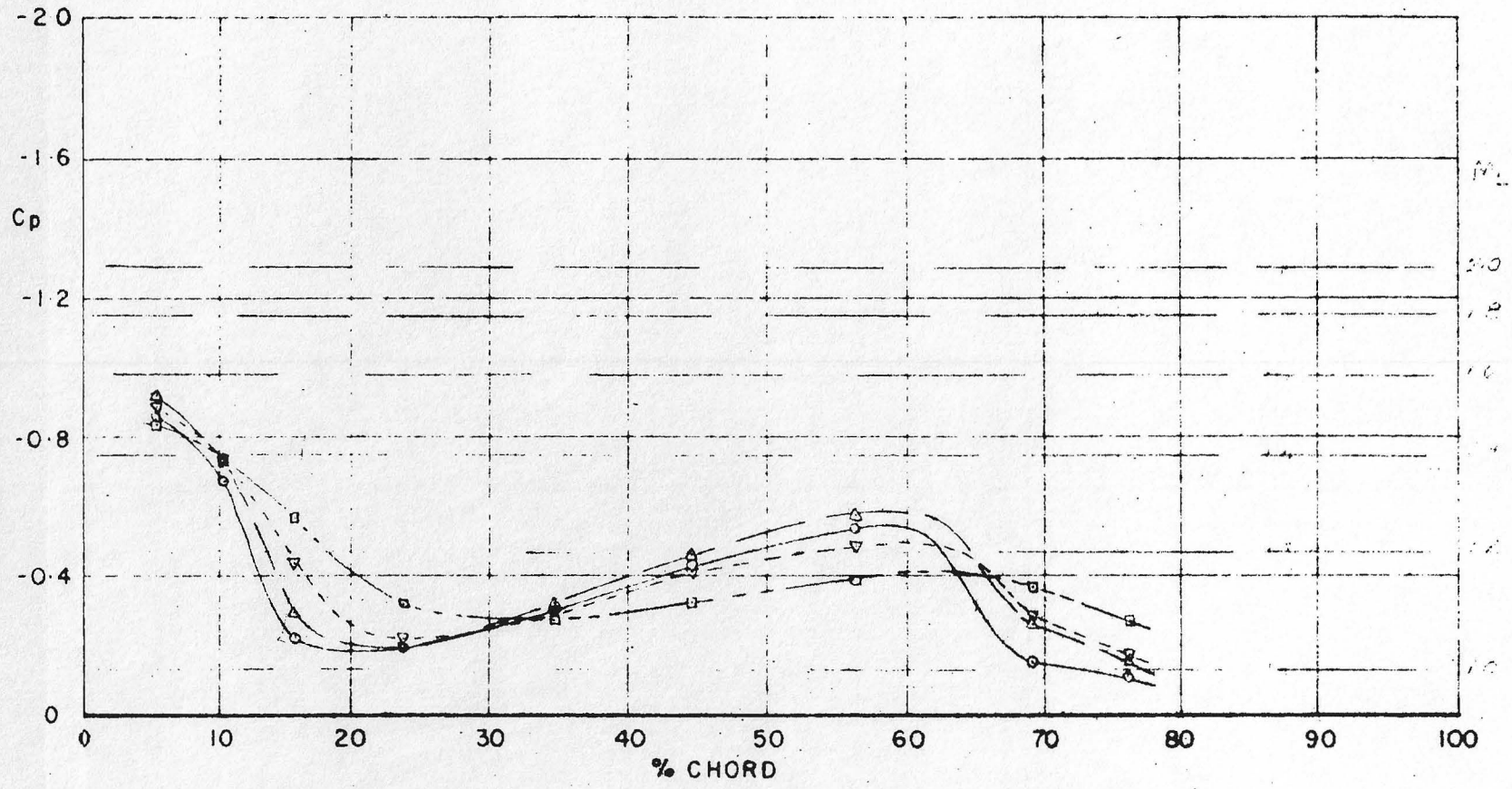

PRESSURE DISTRIBUTION ALONG FUSELAGE-NACELLE FILLET-UPPER SURFACE

M = 0.93

FIG 10

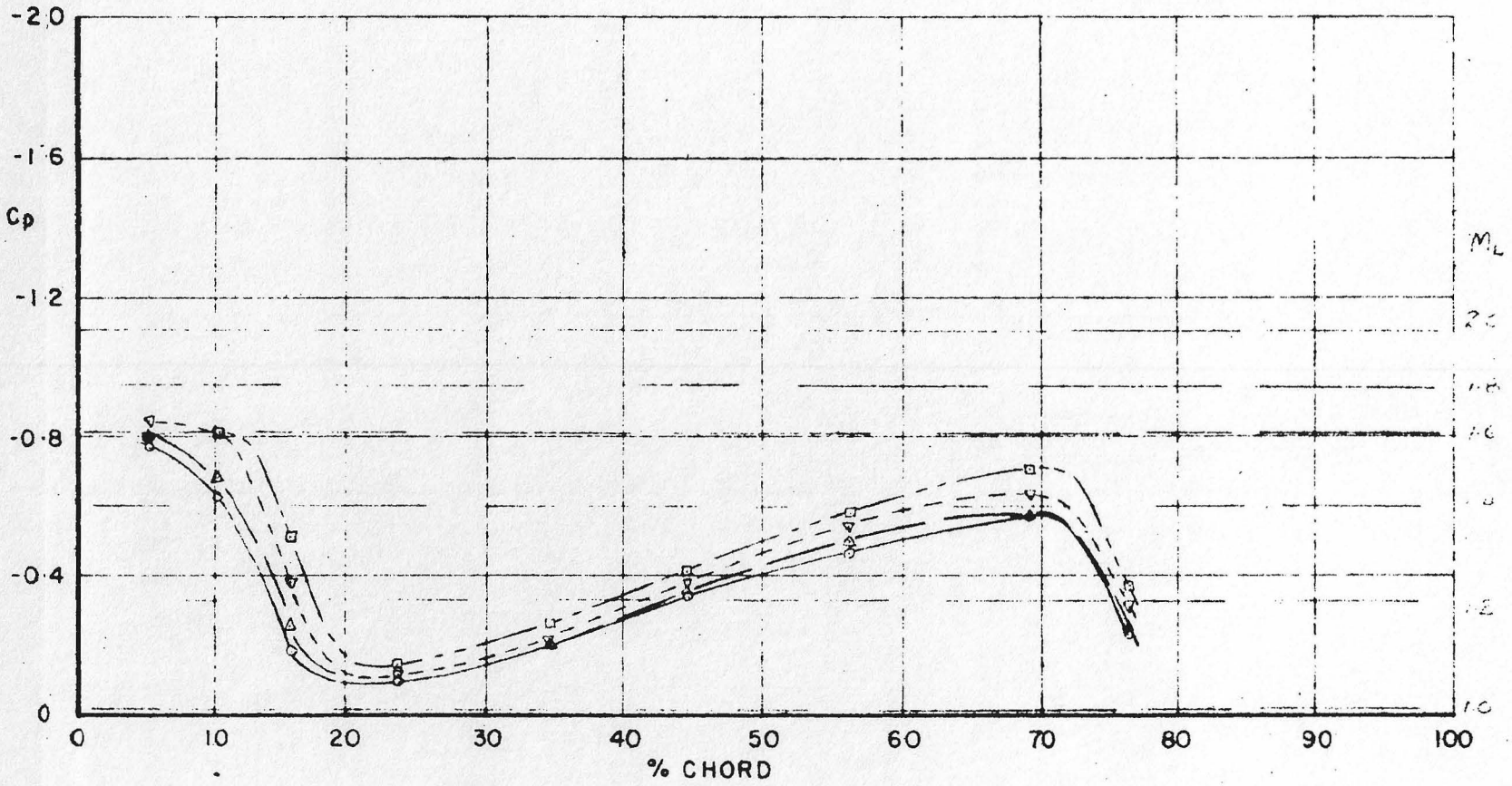

PRESSURE DISTRIBUTION ALONG FUSELAGE-NACELLE FILLET-UPPER SURFACE

M = 0.09

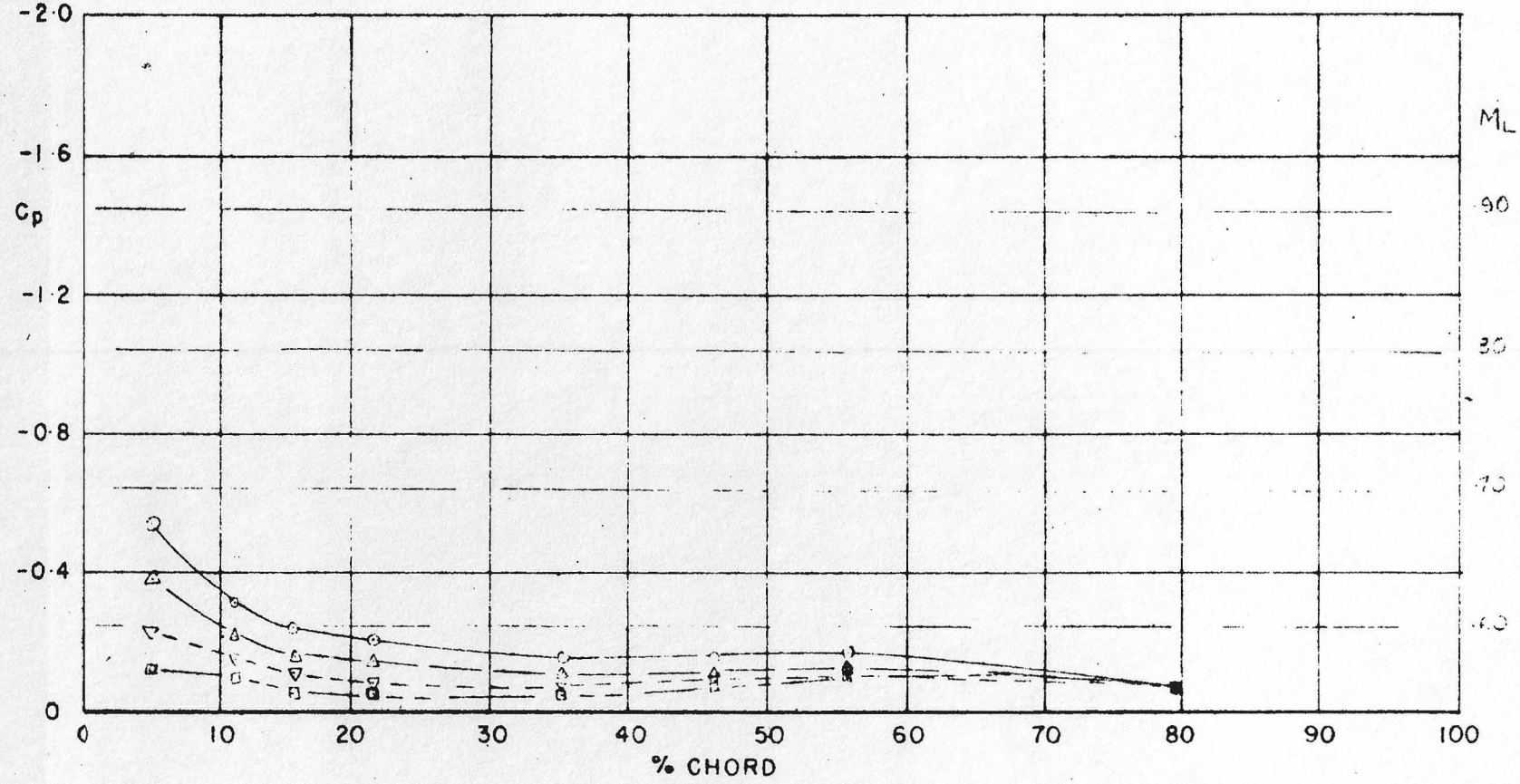

PRESSURE DISTRIBUTION ALONG FUSELAGE-NACELLE FILLET-LOWER SURFACE

M = 0.53

FIG. 21

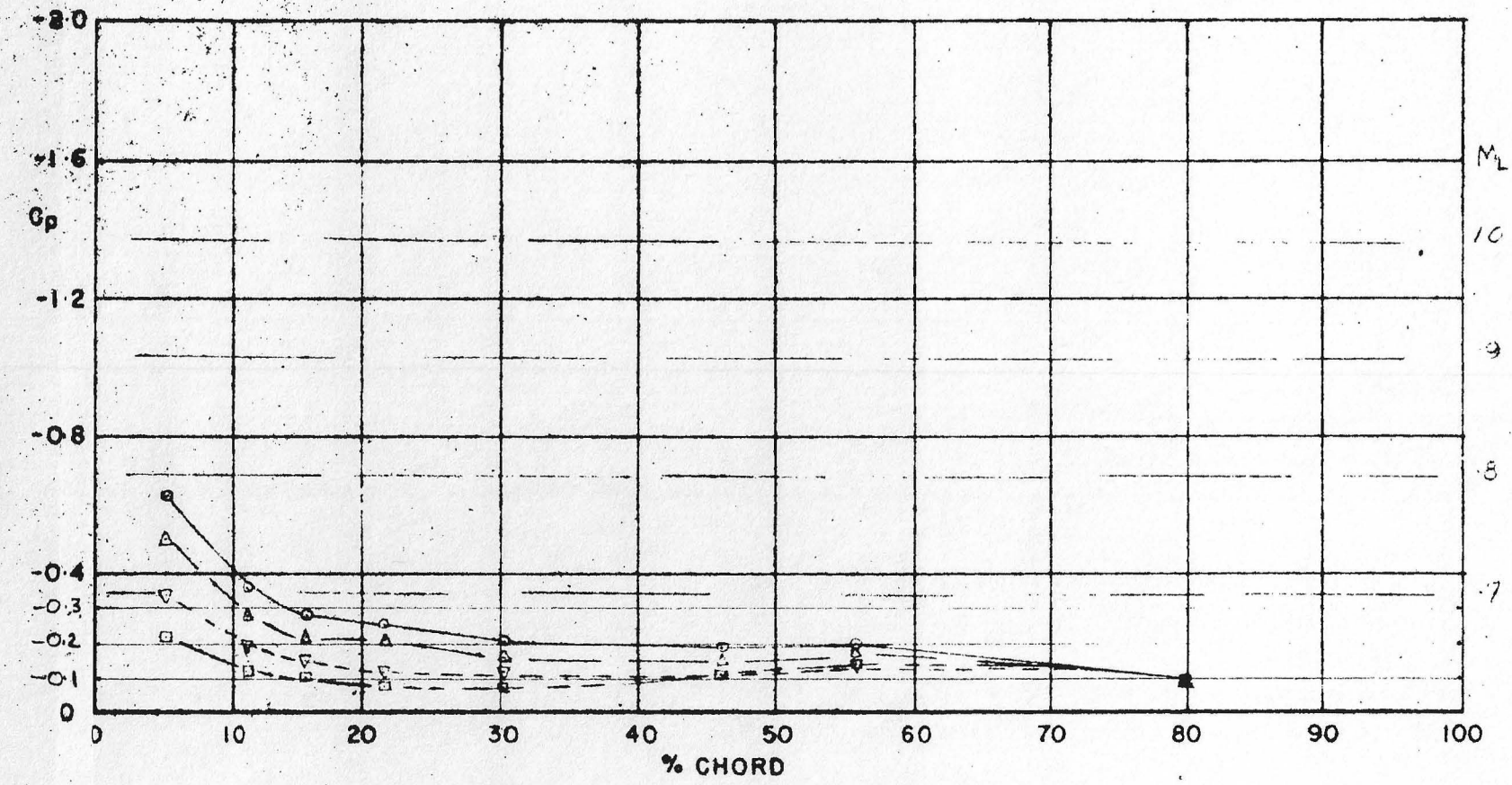

PRESSURE DISTRIBUTION ALONG FUSELAGE-NACELLE FILLET-LOWER SURFACE

M = ·60

FIG 13

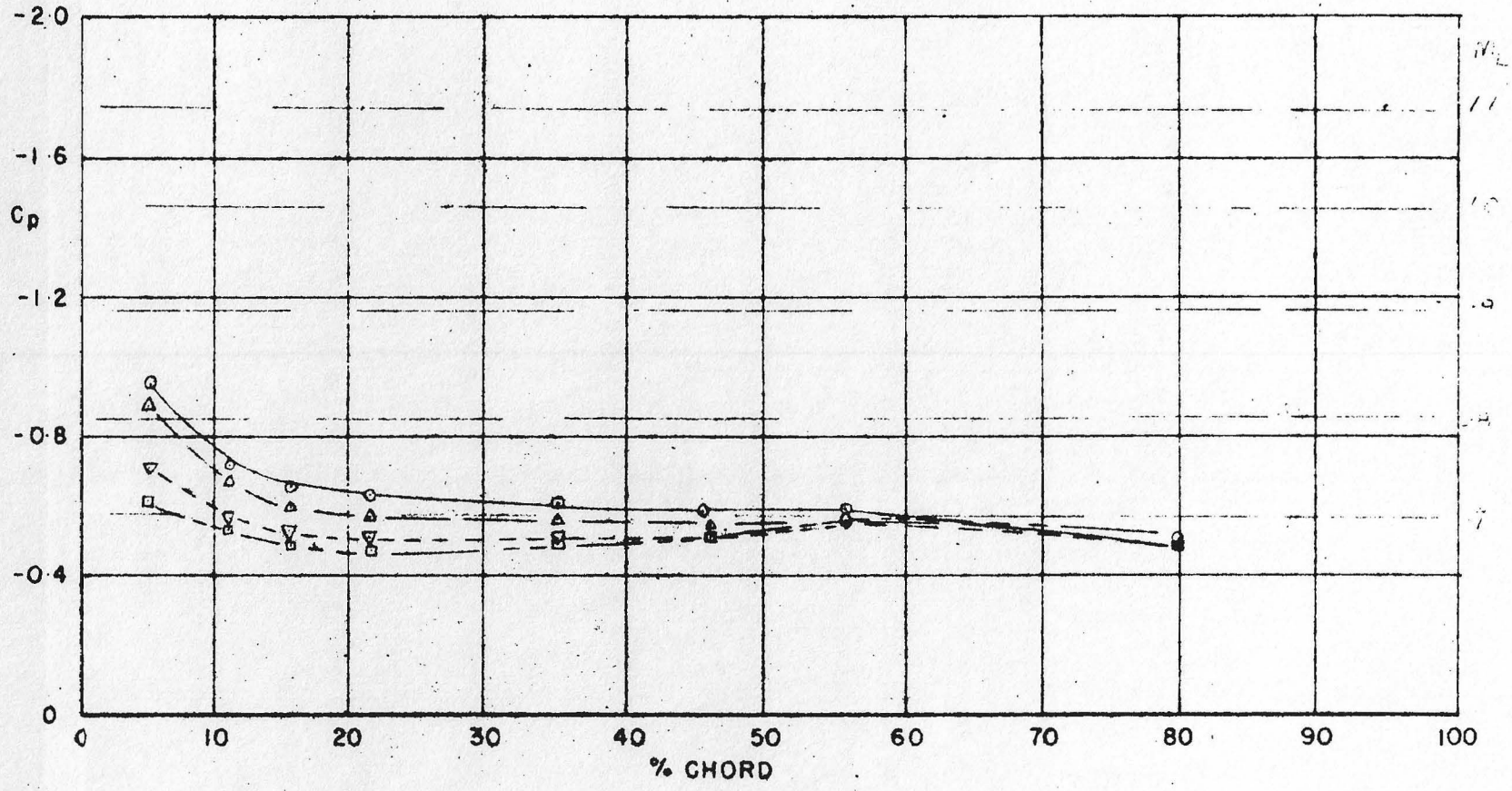

PRESSURE DISTRIBUTION ALONG FUSELAGE-NACELLE FILLET-LOWER SURFACE

M = .65

FIG. 14

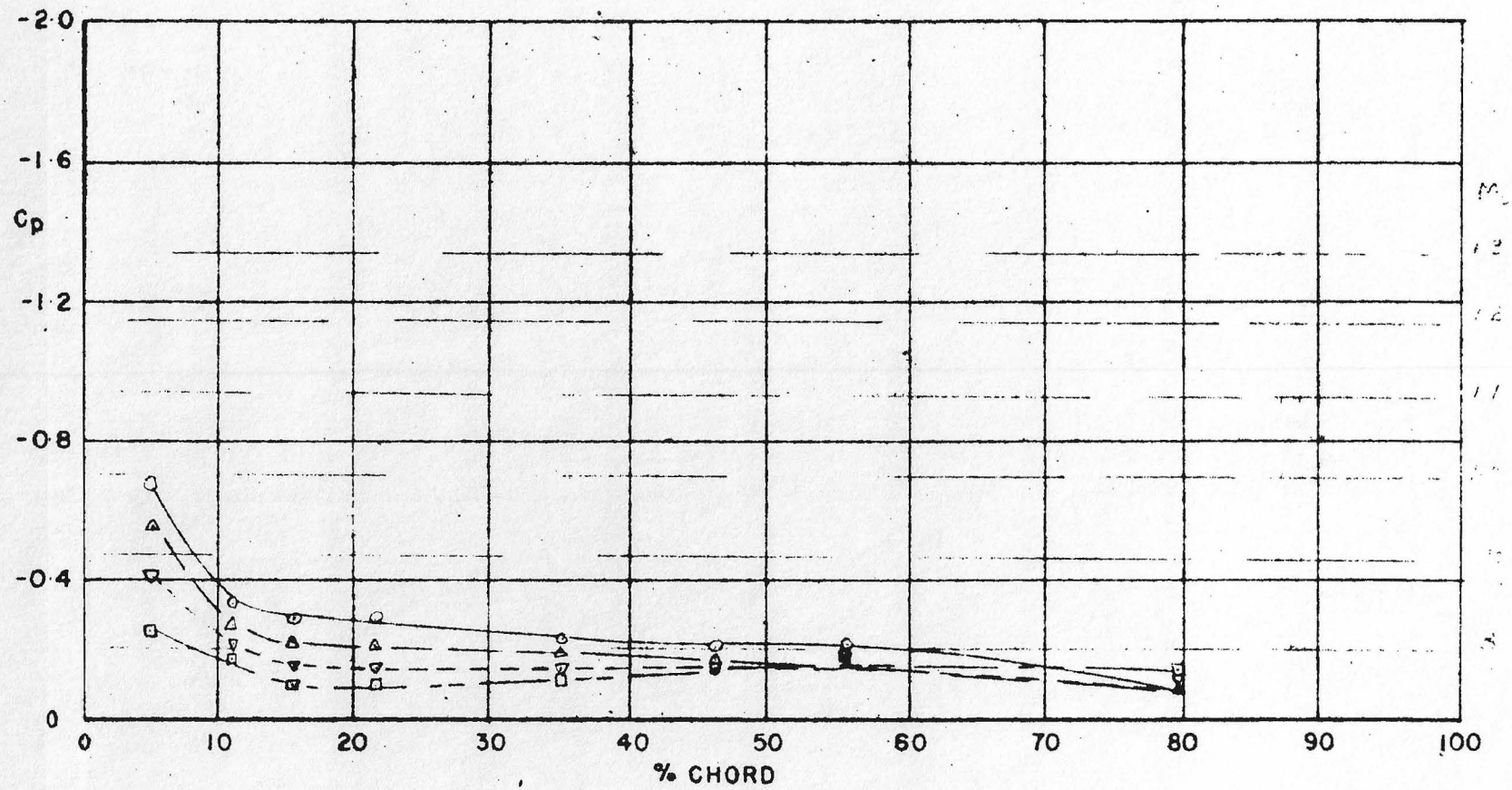

PRESSURE DISTRIBUTION ALONG FUSELAGE-NACELLE FILLET-LOWER SURFACE

M = .72

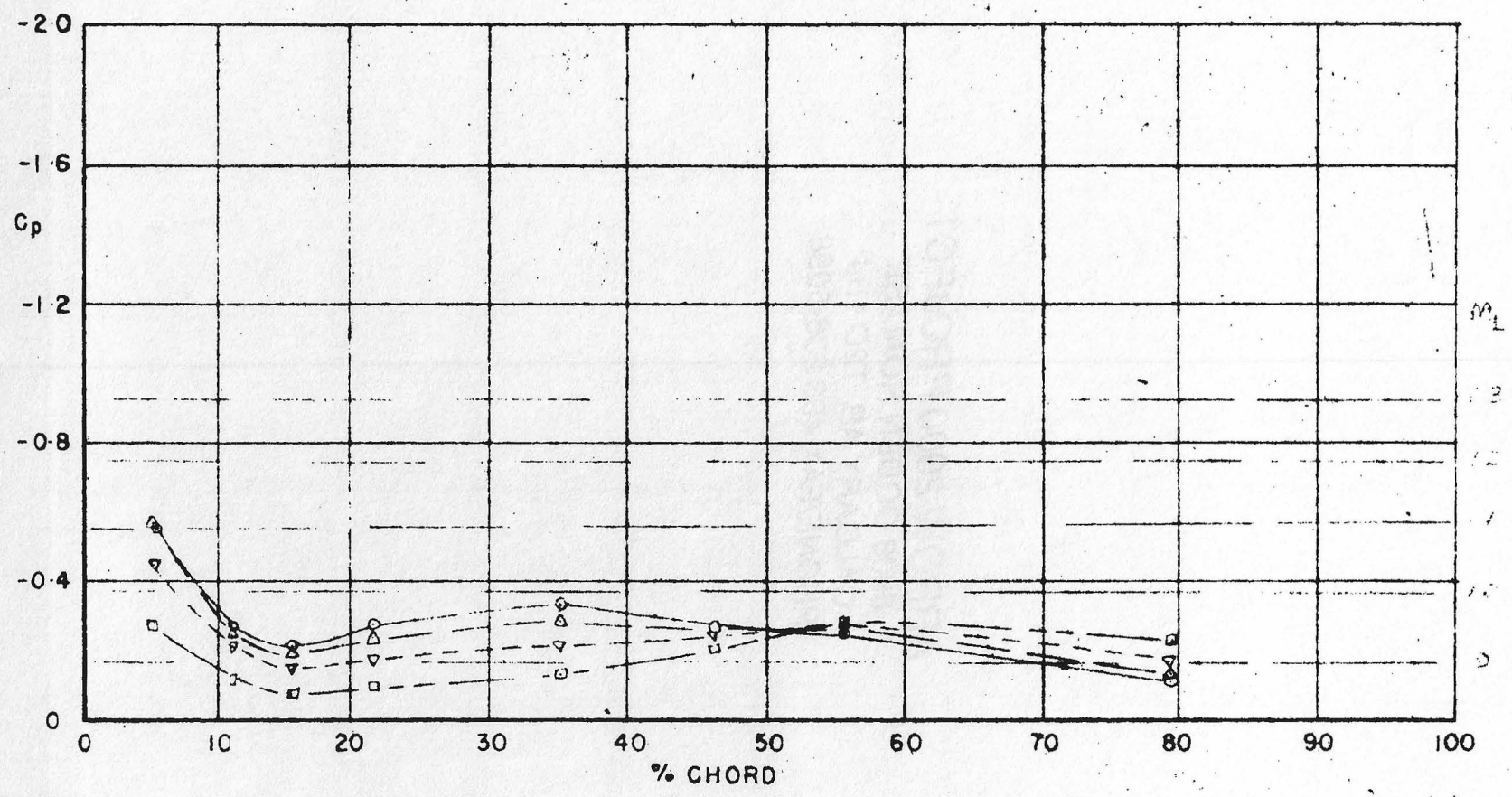

PRESSURE DISTRIBUTION ALONG FUSELAGE-NACELLE FILLET-LOWER SURFACE

M = ·82

Fig. 12